Total-Ionizing-Dose Effects at Ultrahigh Doses in AlGaN/GaN HEMTs

Stefano Bonaldo, *Member, IEEE*, En Xia Zhang, *Senior Member, IEEE*, Serena Mattiazzo, Alessandro Paccagnella, *Senior Member, IEEE*, Simone Gerardin, *Member, IEEE*, Ronald D. Schrimpf, *Fellow, IEEE*, and Daniel M. Fleetwood, *Fellow, IEEE*

***Abstract*— Total-ionizing-dose (TID) effects in AlGaN/GaN high-electron-mobility transistors (HEMTs) are evaluated by dc and low-frequency noise measurements. Devices with and without passivation layers are irradiated with 10-keV X-rays up to 100 Mrad(SiO_2) under different bias conditions. Irradiated devices show significant electrical shifts in threshold voltage and transconductance. At doses <10 Mrad(SiO_2), the TID-induced effects are related to the passivation of preexisting acceptor-like defects via hole capture, which induces negative threshold voltage shifts and improvement of transconductance. At doses >10 Mrad(SiO_2), dehydrogenation of defects and impurity complexes leads to the creation of acceptor-like defects, which degrade the transconductance, shift positively the threshold voltage, and increase the low-frequency noise. Effects are enhanced in unpassivated devices and when the gate is biased at high voltage.**

***Index Terms*— AlGaN high-electron-mobility transistors (HEMTs), bias condition, charge trapping, dc, low-frequency noise, total ionizing dose (TID).**

I. Introduction

THE demands on electronics working in harsh radiation environments have increased in the last several decades. Experimental fusion reactor facilities, nuclear waste depositories, and next-generation particle accelerators require chips able to withstand ultrahigh ionizing radiation doses on the order of >10 Mrad(SiO_2). For example, the trackers of the future High-Luminosity Large Hadron Collider (HL-LHC) at CERN, Switzerland, will be exposed to total ionizing doses (TIDs) up to 1 Grad(SiO_2) over ten years of operation [1].

TID effects at ultrahigh doses above ∼10 Mrad(SiO_2) have been investigated in Si-based planar and FinFET technologies [2], [3], [4], [5], [6], [7], [8], [9], [10], [11], [12]. Studies at 1 Grad(SiO_2) on 65-nm MOSFETs [2], [3], [4], 31-nm MOSFETs [6], [7], [8], 16-nm FinFETs [9], [10], [11], and gate-all-around FETs [12] have revealed issues related to radiation-induced charge buildup in dielectrics, e.g., in shallow trench isolation (STI) and in spacers and have underlined the important role of hydrogen transport for the activation of TID-induced traps.

On the other hand, power and RF systems often incorporate compound semiconductor devices, including GaN-based high-electron-mobility transistors (HEMTs). AlGaN/GaN HEMTs are widely used in high-power and radio frequency applications due to their enhanced carrier mobility in the two-dimensional electron gas (2-DEG) and their high breakdown electric field [13]. The absence of gate dielectrics in AlGaN/GaN devices is a key factor for their high tolerance to ionizing radiation [14]. However, in the last ten years, several works have pointed out significant TID sensitivities of AlGaN/GaN HEMTs; these may prevent the proper functioning at the relatively low doses typical of space applications and are likely to be even larger in high-radiation applications [15], [16], [17], [18], [19], [20], [21], [22], [23].

X-ray and 1.8-MeV proton irradiations revealed that AlGaN/GaN HEMTs often exhibit threshold voltage shifts and reductions in transconductance [15], [16], [17]. These TID and DD effects are related primarily to trap activation and/or neutralization in the AlGaN and GaN layers with strong sensitivities to the bias applied during irradiation [15], [16]. The results of proton irradiations are often complicated to interpret, as they combine TID effects with displacement damage (DD) effects. X-ray irradiations in recent works focused on the exploration of pure TID mechanisms in AlGaN/GaN HEMTs. However, the cumulative dose in these studies is typically <1 Mrad(SiO_2), much lower than the TID often induced by proton irradiations, which is often >10 Mrad(SiO_2) [15], [16], [18]. Hence, the pure TID response of GaN HEMTs at ultrahigh doses is still unknown. Its exploration is useful for improving knowledge of basic degradation mechanisms in GaN-based HEMTs.

This work explores ultrahigh-dose effects in a development-stage AlGaN/GaN HEMT technology through dc and low-frequency noise measurements. The results evidence complex synergies between TID effects and electrical stress, each of which is strongly influenced by applied biases. The largest threshold-voltage shifts are observed for this technology when negative-gate bias is applied during irradiation, i.e., when devices are irradiated in the OFF-state. On the contrary, the largest transconductance degradation occurs under ON-bias

Manuscript received 31 October 2022; revised 14 December 2022 and 9 January 2023; accepted 12 January 2023. Date of publication 18 January 2023; date of current version 16 August 2023. This work was supported in part by the U.S. Air Force Center of Excellence in Radiation Effects under Award FA9550-22-1-0012.

Stefano Bonaldo, Alessandro Paccagnella, and Simone Gerardin are with the Department of Information Engineering, University of Padova, 38134 Padua, Italy (e-mail: stefano.bonaldo@unipd.it).

En Xia Zhang, Ronald D. Schrimpf, and Daniel M. Fleetwood are with the Department of Electrical and Computer Engineering, Vanderbilt University, Nashville, TN 37235 USA.

Serena Mattiazzo is with the Department of Physics and Astronomy, University of Padova, 38134 Padua, Italy, and also with INFN Sezione di Padova, 38134 Padua, Italy.

Color versions of one or more figures in this article are available at https://doi.org/10.1109/TNS.2023.3237179.

Digital Object Identifier 10.1109/TNS.2023.3237179

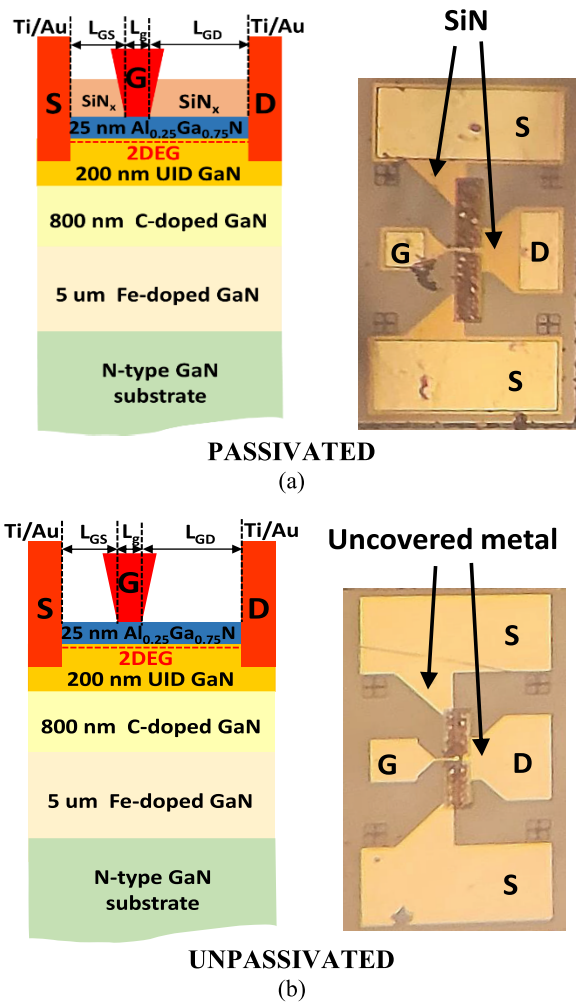

Fig. 1. Schematic diagram of stack layers of AlGaN/GaN HEMTs (not to scale) and optical microscope images of (a) passivated and (b) unpassivated GaN-based HEMTs.

irradiation. Unpassivated devices show larger sensitivity to TID irradiation and bias stress than passivated devices, reinforcing the strong role of hydrogen transport and reactions on the radiation response and reliability of GaN-based HEMTs.

II. Devices and Experimental Details

A. Devices Under Test

The GaN HEMTs under test were fabricated in a development-stage AlGaN/GaN technology at the University of California at Santa Barbara (UCSB), USA [22]. The active region consists of 200 nm of unintentionally doped (UID) GaN that is grown by Ga-rich plasma-assisted molecular beam epitaxy on n-type free-standing GaN substrate having layer doped with Fe and C (Fig. 1). The transistor channel width is 150 μm and the channel length L_g is 0.7 μm, with gate-to-drain separation (L_{gd}) of 1 μm and gate-to-source separation (L_{gs}) of 0.5 μm. Transistors in this study are built in two configurations: 1) passivated by a thick SiN_x layer (normal configuration) and 2) unpassivated (for comparison), as shown in Fig. 1(a) and (b).

TABLE I
Bias Conditions During Irradiation and Annealing*

Bias condition	V_g [V]	V_d [V]	V_s [V]
GND	0	0	0
ON	0	+10	0
CUT-OFF	-7	+10	0
OFF	-7	0	0

*The substrate is always biased at 0 V. The annealing bias condition is identical to the bias condition applied during the irradiation.

B. Test Conditions

Irradiation tests were conducted using a 10-keV X-ray irradiator at a dose rate of 3.8 Mrad(SiO_2)/h for a total exposure time of ~29 h to reach 100 Mrad(SiO_2). All doses and rates are referred to equilibrium doses in SiO_2 for consistency in calibration and to facilitate comparison with other works [15], [16], [17], [18], [19]. Considering the relative atomic numbers, we infer from comparative studies of similar materials that the doses in GaN may be 2×–2.5× the quoted equilibrium SiO_2 dose [24], [25], [26].

The radiation exposure was stopped at several steps. At each step, devices were kept with all terminals grounded for about 60 s before transistors were electrically characterized. This minimizes annealing time and allows the device to stabilize before measurements. After completion, devices were annealed at room temperature (RT) for 27 h. Several bias configurations were applied to the HEMTs during irradiation and annealing, as shown in Table I. The dc static response and low-frequency noise of the transistors were measured at RT before exposure and at several irradiation steps. At least two devices were tested for each set of conditions; the representative results are shown below. The threshold voltage $V_{th}$is defined as $V_{gs-int} - V_{ds}/2$; $V_{gs,int}$ is extracted in the linear region ($V_{ds} = 0.1$ V) as the gate-voltage axis intercept of the linear extrapolation of the $I_d - V_{gs}$ curve at the point of its maximum first derivative.

C. Evaluation of Electrical Stress Effects

Irradiations up to 100 Mrad(SiO_2) require about ~29 h. To distinguish degradation induced by electrical stress from that induced by irradiation, the GaN-based HEMTs were stressed without X-ray under the bias conditions of Table I for the same amount of time required for devices to be irradiated up to 100 Mrad(SiO_2).

Fig. 2 shows the electrical stress-induced degradation for (a) passivated and (b) unpassivated devices irradiated in "CUT-OFF"-bias condition, which is the case in which the largest parametric shifts are observed. The stressed HEMTs exhibit increases in leakage current and shifts of threshold voltage V_{th}. The V_{th} undergoes a negative and rapid shift in the first 1 h. After ~29 h, the passivated HEMT biased in the "CUT-OFF" condition shows an increase of maximum drain current of 4%, while the passivated HEMT shows a decrease of maximum ON-current of 7%. For all biases, the unpassivated HEMTs show greater degradation than passivated devices.

Often electrical-stress-induced effects of HEMTs may be substantial and comparable to the TID-induced effects. For this

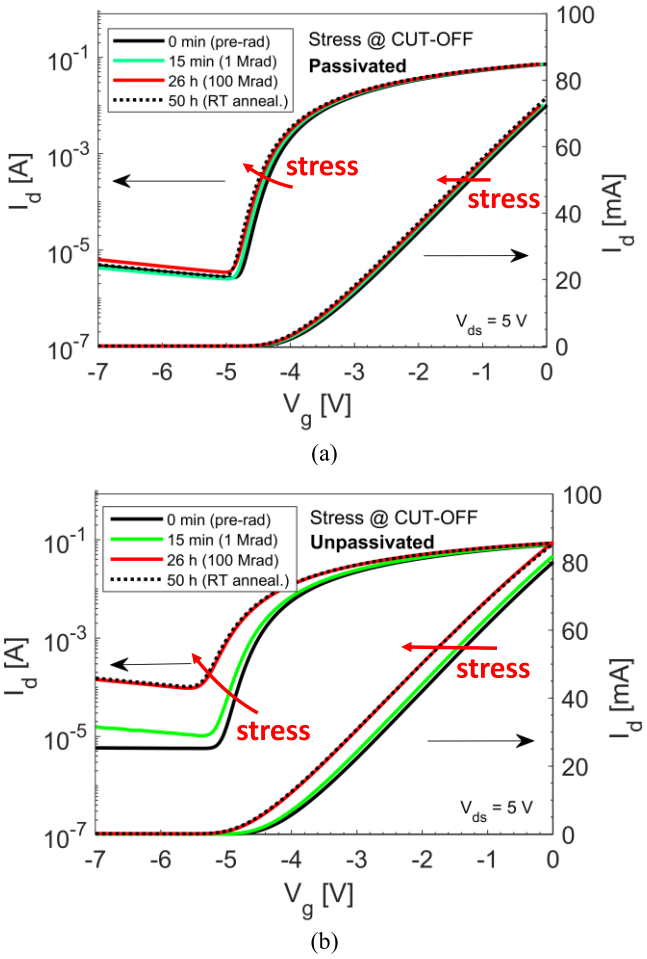

Fig. 2. Electrical stress-induced degradation of I_d–V_{gs} curves in the saturation regime (V_{ds} = 5 V) for (a) passivated and (b) unpassivated AlGaN HEMTs. The devices were biased for a total time of 50 h at RT in the cut-off bias, to evaluate the degradation induced by the electrical stress without X-ray exposure.

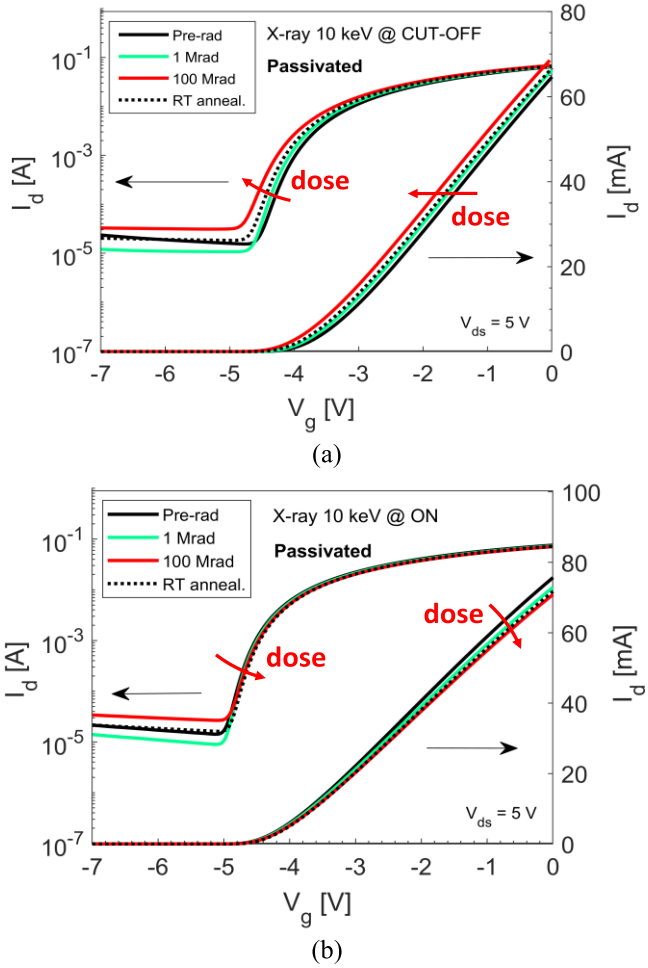

Fig. 3. I_d–V_{gs} curves of passivated GaN-based HEMTs in the saturation regime (V_{ds} = 5 V). The devices were irradiated up to 100 Mrad(SiO_2) and then annealed at RT for 27 h in (a) "CUT-OFF"-bias and (b) "ON"-bias.

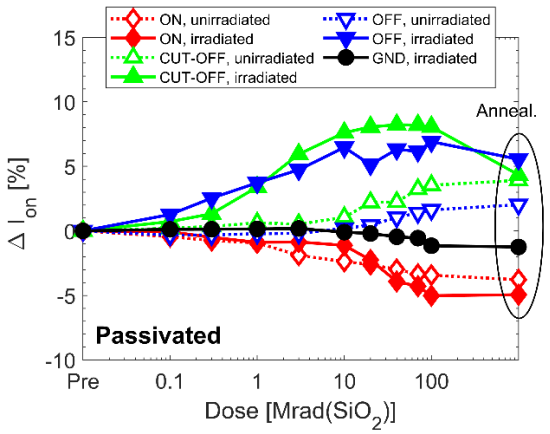

Fig. 4. Degradation of maximum drain current ΔI_{on} as a function of dose in passivated GaN-based HEMTs. Dotted lines refer to the electrical stress-induced degradation, where devices were tested without X-ray exposure; continuous lines refer to test results with X-ray exposure. Irradiations were performed up to 100 Mrad(SiO_2) and then devices were annealed at RT for 27 h in different bias conditions.

reason, Sections III and IV report and compare the responses of biased irradiated and unirradiated devices at similar times.

III. Passivated Devices

A. TID Tolerance at Different Bias Conditions

The dc characteristics in the saturation regime (V_{ds} = 5 V) of passivated GaN-based HEMTs are shown in Fig. 3 when devices are irradiated and annealed under the "CUT-OFF" and "ON"-bias conditions. During exposure, the drain leakage current at V_g = 0 V increases significantly regardless of the applied bias, a signature of drain-to-gate leakage. The V_{th} shifts monotonically to negative values as large as −270 mV in "CUT-OFF"-biased devices and to positive values up to 50 mV in "ON"-biased devices. The "ON"-biased devices exhibit degradation of the transconductance g_m, which is evident as decreases in the slopes of the $I_d - V_g$ curves for –3 V < V_g < 0 V. Slight performance recovery is visible after 27 h of RT annealing, suggesting the formation of a significant density of stable defects.

Fig. 4 shows the effects of applied bias on the degradation of the maximum drain current I_{on}, defined here as the drain current at V_{gs} = 0 V and V_{ds} = 5 V. Dotted lines refer to electrical-stress-induced degradation without X-ray exposure; continuous lines are obtained with X-ray

exposure. GaN HEMTs irradiated in the "CUT-OFF" and "OFF" biases show increases (improvement) in I_{on} by about 9% and 7% at 100 Mrad(SiO_2). RT annealing reduces this increase: $\Delta I_{on} = 4\%$ after 27 h. The significant difference between the continuous and dotted lines demonstrates that the performance enhancement of "CUT-OFF" and "OFF"-biased devices is affected more strongly by TID-induced effects than by bias-induced effects. On the contrary, devices irradiated in the "ON"-bias condition exhibit a degradation, as evidenced by the 5% decrease of I_{on} at 100 Mrad(SiO_2). The degradation for devices irradiated or electrically stressed in the "ON"-bias condition is similar, showing that bias-induced stress dominates the changes in device response.

Fig. 5 shows the radiation-induced degradation of the dc parameters (a) ΔV_{th} and (b) maximum transconductance Δg_{m-MAX}, calculated in the linear regime at $V_{ds} = 0.5$ V. These values are for different GaN-based HEMTs irradiated and then annealed under different bias conditions. The I_{on} variation of irradiated GaN HEMTs of Fig. 4 is dominated by the negative shift of $V_{th}$for "CUT-OFF" and "OFF"-biased devices. Three interesting effects are evident in Fig. 5 as follows.

1) Insensitivity to TID When Irradiated at 0-V Gate Bias: The best TID tolerance is found for "GND"-biased and "ON"-biased devices, for which the gate bias is 0 V. This enhancement of the TID tolerance is most likely related to the limited charge yield at low electric fields [15], [16], [27]. The "ON"-biased devices show a slight V_{th} increase and g_m decrease, but this degradation is related to a bias-stress-induced effect, as shown by the overlapping of the continuous and dotted (red) curves. It is more likely that "ON"-biased devices suffer from hot-electron stress, which can induce the activation of acceptor-like traps through the dehydrogenation of O_N–H complexes in the GaN buffer layer [15], [17], [19]. In the case of "ON"-biased devices, post-irradiation annealing continues to induce a slight increase of the V_{th}, as "ON" bias is maintained for longer times.

2) Rebound of the V_{th} Shifts at 10 Mrad(SiO_2) of Irradiated HEMTs: Irradiations in the "CUT-OFF" and "OFF" conditions induce an initial negative V_{th}shift. At 10 Mrad(SiO_2), the ΔV_{th} is about –280 mV for the "CUT-OFF"-biased HEMTs and –263 mV for "OFF"-biased HEMTs. The negative V_{th} shift and the increase of g_{m-MAX} indicate the neutralization of acceptor-like defects [28]. After 10 Mrad(SiO_2), V_{th} recovers somewhat, as shown by the positive trend versus dose. At 100 Mrad(SiO_2), ΔV_{th} is about –190 mV for both "CUT-OFF and "OFF"-biased HEMTs and it continues to recover during the RT annealing.

3) Rebound of g_{m-MAX} at 10 Mrad(SiO_2) of Irradiated HEMTs: At doses <10 Mrad(SiO_2), the g_{m-MAX} of irradiated HEMTs increases with cumulative dose at a higher rate compared to electrically stressed devices, consistent with accelerated acceptor neutralization [17]. At doses >10 Mrad(SiO_2), g_{m-MAX} degrades, suggesting activation of defects in the active GaN layer [15], [17], [19]. Increases of acceptor-like defect densities in the 2-DEG may lead to TID-induced transconductance loss and positive V_{th} shifts, i.e., formation of N vacancies, Ga vacancies, and/or O_N DX centers [15], [16], [18], [20], [29].

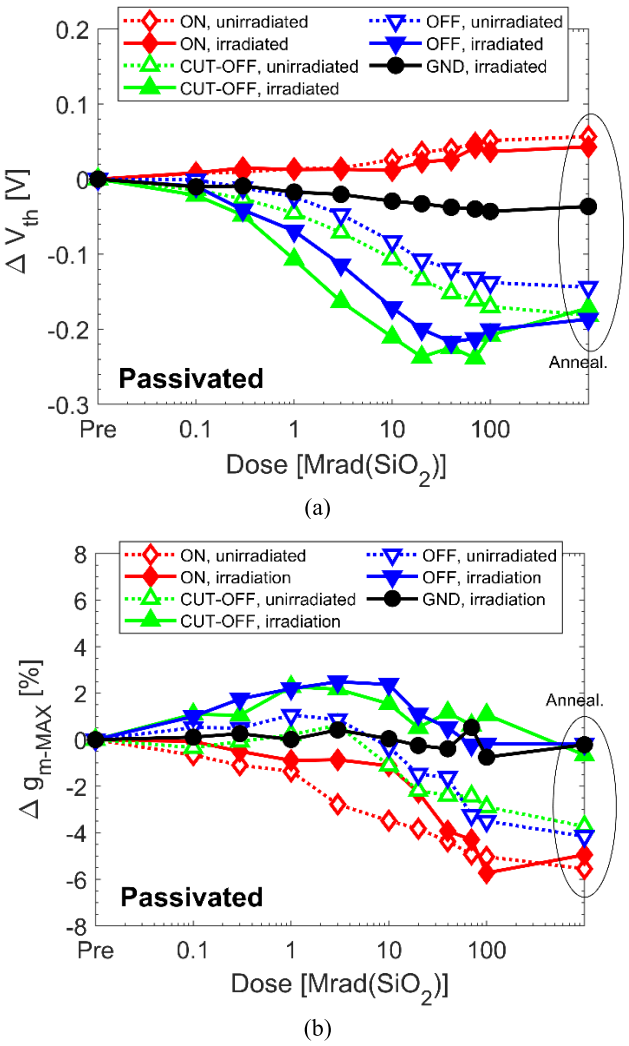

Fig. 5. Degradation of (a) threshold voltage ΔV_{th} and (b) maximum transconductance Δg_{m-MAX} as a function of dose in passivated GaN-based HEMTs. Dotted lines refer to electrical stress-induced degradation without X-ray exposure; continuous lines refer to test results with X-ray exposure. Irradiations were performed up to 100 Mrad(SiO_2); then, devices were annealed at RT for 27 h in different bias conditions.

B. Low-Frequency Noise Responses

Additional insight into densities of defects contributing to charge trapping are obtained by low-frequency noise measurements [15], [16], [18], [30], [31], [32], [33]. The drain-voltage noise power spectral density S_{vd} was evaluated in a frequency span between 1 Hz and 1 kHz at $|V_{ds}| = 0.1$ V for several values of $V_{gt} = V_{gs}–V_{th}$. The low-frequency noise of GaN-based HEMTs is caused primarily by fluctuations of the number of carriers induced by the capture and emission of carriers at individual defect sites in the GaN layer or at the AlGaN/GaN border, which is often affected by the atomic reconfiguration of single-defect sites in the GaN [27], [29].

Fig. 6 shows the low-frequency noise for (a) "CUT-OFF"-biased and (b) "ON"-biased HEMTs before irradiation, at 1 Mrad(SiO_2), at 100 Mrad(SiO_2), and after

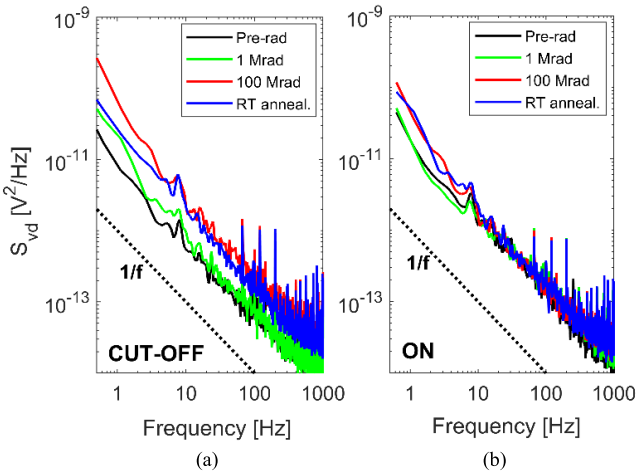

Fig. 6. Low-frequency noise magnitudes for GaN-based HEMTs irradiated and annealed in (a) "CUT-OFF"-bias condition and (b) "ON"-bias condition. The noise was measured at $V_{ds} = 0.5$ V and $V_{gt} = 0.6$ V at RT.

high-temperature annealing. GaN-based HEMTs show typical $1/f$ low-frequency noise. In "ON"-biased HEMTs, the noise is constant and is relatively insensitive to the irradiation and electrical stress. On the other hand, the noise magnitude of "CUT-OFF"-biased devices is approximately constant at 1 Mrad(SiO_2) and increases at 100 Mrad(SiO_2). This increase of the noise, which is visible only at ultrahigh doses, indicates activation of new traps, in agreement with the V_{th} increases and g_m decreases occurring at >10 Mrad(SiO_2) in Fig. 5. During RT annealing, very little change occurs to the noise.

To investigate the density distributions in space and energy of the border traps, Fig. 7 plots the low-frequency noise magnitude at 10 Hz as a function of $V_{gt} = V_{gs} - V_{th}$ in GaN-based HEMTs irradiated in "CUT-OFF" and "ON"-bias conditions. When the slope $|\beta|$ of the $S_{vD} - V_{gt}$ curve is approximately equal to 2, the effective density of the border traps is uniform in space and energy [27], [28], [29], [33], [34]. "CUT-OFF"-biased devices show a significant increase of low-frequency noise levels at 100 Mrad(SiO_2) in agreement with Fig. 6(a). In both pristine and irradiated devices, the slope $|\beta|$ of S_{vd}–$V_g t$ is ~2.1, indicating an approximately uniform spatial and energetic distribution of traps [27], [28], [29]. The slope $|\beta|$ of S_{vd}-V_{gt} is ~2.5 after the RT annealing, suggesting a less uniform density of generated traps in space and energy. On the other hand, "ON"-biased devices are characterized by constant noise with $|\beta|$ equal to 2, indicating uniform and constant density of traps. RT annealing in "ON"-biased devices induces a slight increase in $|\beta|$, which is equal to 2.3 after 27 h of RT annealing.

IV. Unpassivated Devices

A. TID Sensitivity

This section analyzes the TID response of unpassivated devices that are otherwise similar to those in Figs. 3–7. The dc characteristics in the linear regime ($V_{ds} = 0.1$ V) of unpassivated GaN-based HEMTs are shown in Fig. 8 when the devices are irradiated and annealed in the "CUT-OFF" and

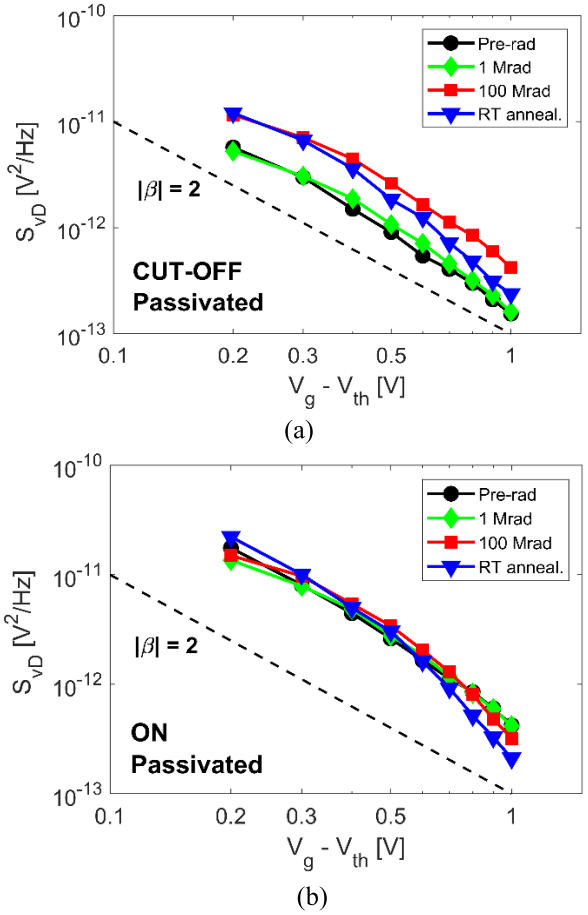

Fig. 7. $1/f$ noise magnitudes at $f = 10$ Hz versus V_{gs}–V_{th} at $V_{ds} = 0.5$ V for GaN-based HEMTs with irradiated and annealed in (a) "CUT-OFF"-bias condition and (b) "ON"-bias condition.

"ON"-bias conditions. The highest shift is visible in the "CUT-OFF" condition, where V_{th} shifts to negative values by about ~0.6 V and the leakage current increases by two orders of magnitude, from 2×10^{-6} to 2×10^{-4} A. Slight performance recovery is visible after 27 h of RT annealing, similar to passivated devices. The "ON"-biased devices are characterized by negative V_{th} shifts, about –270 mV after 100 Mrad(SiO_2), which are smaller than those of "CUT-OFF"-biased devices.

The influence of irradiation bias on TID sensitivity is shown in Fig. 9, which summarizes the degradation of: (a) maximum drain current I_{on}, (b) threshold voltage V_{th}, and (c) maximum transconductance g_{m-MAX}. The dotted lines refer to electrical stress-induced degradation without X-ray exposure; continuous lines are obtained with X-ray exposure. The I_{on} variation of irradiated GaN HEMTs of Fig. 9(a) is mostly dominated by the negative shift of V_{th}. The highest shift is visible in "CUT-OFF" and "OFF" biases, while the bias conditions with the smallest degradation are the "GND" and "ON" conditions. The clear separation of dotted and continuous lines indicates that the degradation induced during the exposure is mainly related to TID.

In contrast to the passivated HEMTs, the V_{th} values of unpassivated devices irradiated in "GND" and "ON" conditions degrade with a similarly decreasing monotonic trend.

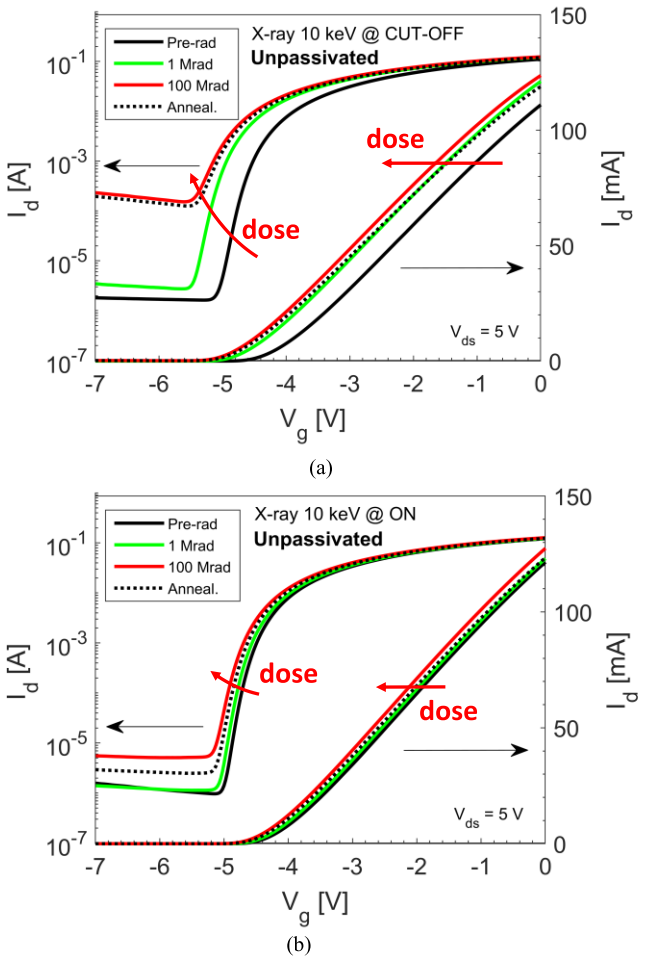

Fig. 8. I_d–V_{gs} curves of unpassivated GaN-based HEMTs in the saturation regime (V_{ds} = 5 V). The devices were irradiated up to 100 Mrad(SiO_2) and then annealed at RT for 27 h in (a) "CUT-OFF"-bias and (b) "ON"-bias.

On the other hand, similar to passivated devices, the "CUT-OFF" and "OFF"-biased transistors exhibit a rebound of the V_{th} and g_m values around 10 Mrad(SiO_2). At doses <10 Mrad(SiO_2), V_{th} shifts to negative values and g_m increases. At doses >10 Mrad(SiO_2), V_{th} shifts toward more positive values and g_m decreases.

Fig. 10 shows ΔV_{th} as a function of the time for devices that were irradiated in the OFF-bias condition and then annealed at RT for up to 24 h in the same bias condition. In the passivated devices, V_{th} recovers by 34 mV in the first 5 h and by 40 mV after 24 h. In unpassivated devices, V_{th} recovers by 79 mV in the first 5 h and by 103 mV after 24 h. The plot shows that most annealing-induced shifts occur in the first 5 h with the highest shifts in unpassivated devices. The recovery then saturates, becoming approximately stable for annealing times over 15 h. The additional annealing that occurs in the unpassivated devices is most likely due to enhanced hydrogen diffusion and passivation reactions in these devices [21], [23], as discussed in Section V.

Low-frequency noise measurements for the "CUT-OFF"-biased HEMTs show typical $1/f$ low-frequency noise, as shown in Fig. 11(a). The noise magnitude was unchanged up to 1 Mrad(SiO_2) and increased by almost one order of magnitude after 100 Mrad(SiO_2), indicating activation of new border traps. Fig. 11(b) plots the low-frequency noise magnitude at 10 Hz as a function of Vgt in the HEMTs irradiated in "CUT-OFF"-bias condition. The devices show significant increases of the low-frequency noise levels at 100 Mrad(SiO_2), corresponding to the V_{th} increase and g_m decrease visible in Fig. 11. In both pristine and irradiated devices, the slope $|\beta|$ of Sid–Vgt is ~2.1 indicating an approximately uniform spatial and energetic distribution of traps [27], [28], [29] before and during the irradiation. During RT annealing, the value of $|\beta|$ is 2.4, indicating a slightly non-uniform redistribution of the traps.

B. TID Mechanisms

These results suggest two main TID-related mechanisms as follows.

- *First Mechanism:* This is characterized by negative V_{th} shifts, g_m increases, and unchanged noise. In unpassivated devices, this response is visible under all bias conditions, with enhancement at high gate biases. It is likely that this mechanism results from the TID-assisted passivation of acceptor-like defects via hole capture [16], [32].

- *Second Mechanism:* This is characterized by positive V_{th} shifts, g_m degradation, and the increase of the low-frequency noise magnitude. It is visible only during the irradiation at high gate biases, i.e., "CUT-OFF" and "OFF" at doses >10 Mrad(SiO_2). It is more likely that this mechanism is related to the activation of acceptor-like defects via dehydrogenation of defects, as often observed in proton-irradiated GaN-based HEMTs at higher fluences [15], [16], [18], [29].

C. Leakage Current

Fig. 12 plots the OFF-state leakage current I_{off} flowing through the drain terminal when V_{gs} = –7 V and V_{ds} = 5 V in unpassivated HEMTs. In general, the value of I_{off} increases by about one order of magnitude after devices are irradiated to 100 Mrad(SiO_2), with negligible contributions of electrical stress (dotted curves). Only GaN-based HEMTs in the "CUT-OFF"-bias condition (green curves) exhibit these large I_{off} increases of about two orders of magnitude. This high I_{off} degradation in "CUT-OFF"-biased HEMTs is induced by electrical stress, which is enhanced when the gate and drain are simultaneously biased at opposite voltages. The high electric field induced by high gate-to-drain voltage may lead to percolation-based transport through defect and/or impurity centers in the AlGaN layer [20], [29], [35], [36], [37]. Particularly at higher voltages, these stress conditions may also lead to impact ionization of carriers, leading to positive charge trapping in the passivation layer of these devices [37], [38].

V. Discussion

Fig. 13 shows the ΔV_{th} and gate leakage I_g of passivated and unpassivated HEMTs irradiated and annealed under different bias conditions. The "CUT-OFF" and "OFF"-biased HEMTs have similar TID responses; only "CUT-OFF"-biased devices are shown for clarity. The trends of curves in Fig. 13(a)

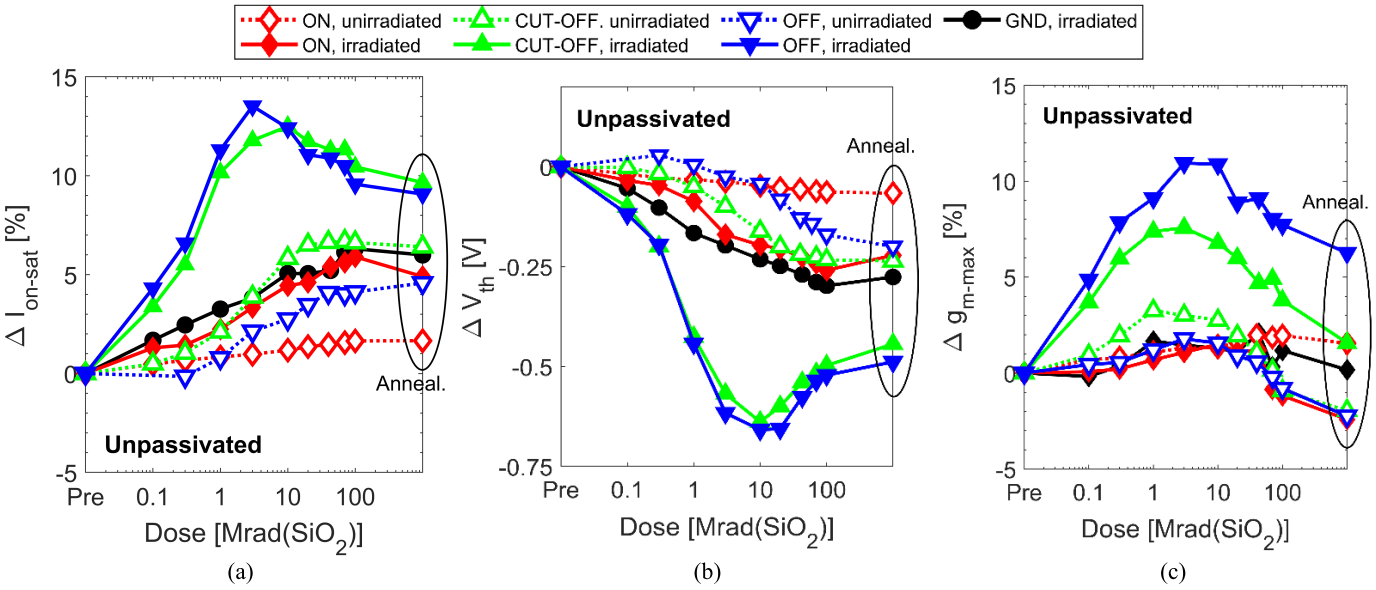

Fig. 9. Degradation of (a) maximum drain current $\Delta I_{\text{on-lin}}$, (b) threshold voltage ΔV_{th}, and (c) maximum transconductance $\Delta g_{m-\text{MAX}}$ as a function of dose in unpassivated GaN-based HEMTs. Dotted lines refer to electrical-stress-induced degradation, where devices were tested without X-ray exposure; continuous lines refer to test results with X-ray exposure. Irradiations are performed up to 100 Mrad(SiO_2), and then devices were annealed at RT for 27 h in different bias conditions.

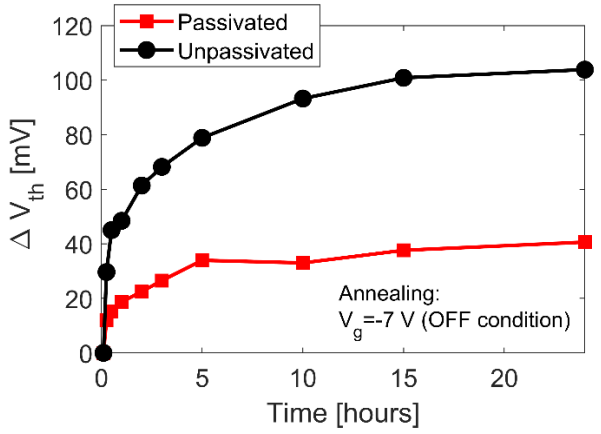

Fig. 10. Change in threshold voltage ΔV_{th} versus time in passivated and unpassivated GaN-based HEMTs. The ΔV_{th} is measured during RT annealing of devices that were irradiated to 100 Mrad(SiO_2). The annealing is performed at $V_g = -7$ V, i.e., in the OFF-bias condition.

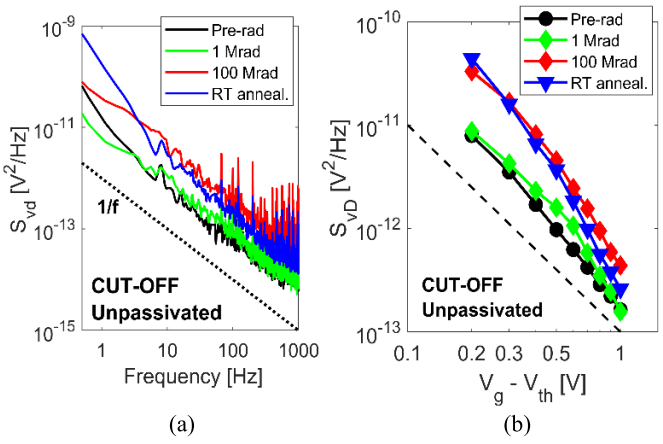

Fig. 11. (a) Low-frequency noise magnitudes for unpassivated GaN HEMTs irradiated in the "CUT-OFF"-bias condition. The noise was measured at $V_{\text{ds}} = 0.1$ V and $V_{\text{gt}} = 0.5$ V at RT. (b) $1/f$ noise magnitudes at $f = 10$ Hz versus V_{gs}–V_{th} at $V_{\text{ds}} = 0.1$ V for the "CUT-OFF" irradiated HEMT.

among passivated and unpassivated devices are generally similar, except for passivated "ON"-biased devices, for which the degradation is dominated by electrical stress. TID-induced effects are enhanced when bias is applied to the gate, i.e., at $V_g = -7$ V, corresponding to the OFF-condition. In "CUT-OFF" passivated and unpassivated devices, TID effects are caused by the two mechanisms described in Section IV. The first mechanism occurs at doses <10 Mrad(SiO_2) with negative V_{th} shifts, while the second mechanism dominates at doses >10 Mrad(SiO_2) with positive V_{th} shifts. "GND" and "ON"-biased devices exhibit only the first mechanism, inducing negative V_{th} shifts.

Observed shifts in Fig. 13(a) are smaller for passivated devices than unpassivated devices. After 100 Mrad(SiO_2) in the "CUT-OFF"-bias condition, V_{th} values for the passivated HEMTs shift by –0.34 V versus –0.68 V for unpassivated devices. The higher TID sensitivity of unpassivated HEMTs compared to passivated devices highlights the key role of contaminant absorption (e.g., oxygen, moisture) through the surface layers [21], [23]. SiN_x passivation inhibits moisture absorption, limiting the formation of acceptor-like defects [21]. Hence, the composition and thickness of passivation layers are the important factors in determining the radiation tolerance and long-term reliability of GaN-based HEMTs.

Fig. 13(b) shows the gate current I_g normalized by its pre-irradiation value of I_{g0} for GaN-based HEMTs irradiated under different bias conditions. In general, the highest gate-to-drain leakage currents are visible in unpassivated devices. After 100 Mrad(SiO_2), the value of I_g/I_{g0} of unpassivated HEMTs increases by roughly one order of magnitude for

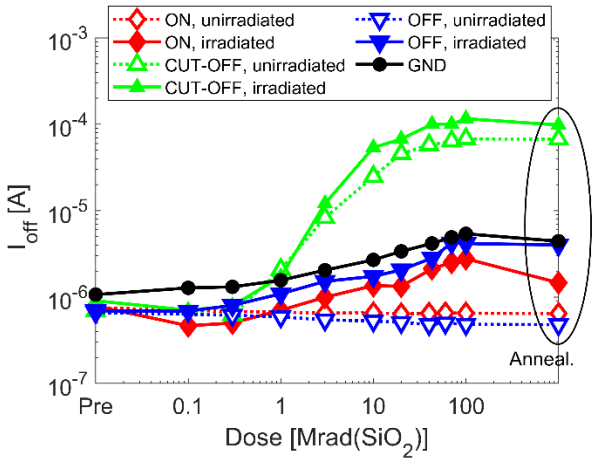

Fig. 12. Increase of the drain leakage current I_{off} at $V_{ds} = 5$ V as a function of cumulative dose for GaN HEMTs irradiated and annealed in different bias conditions.

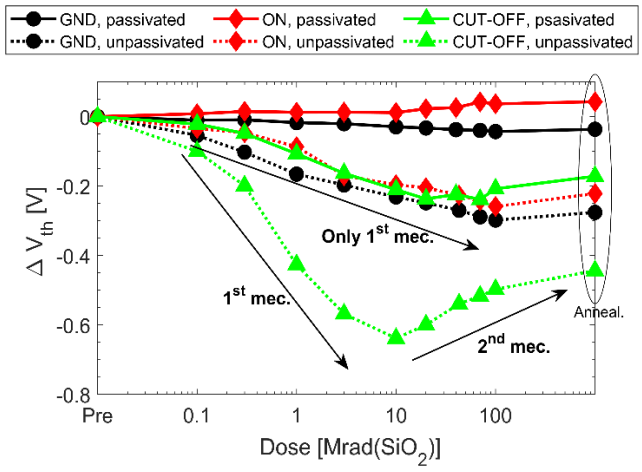

(a)

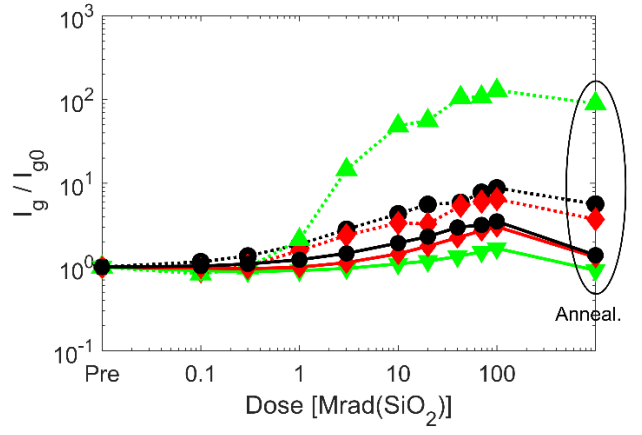

(b)

Fig. 13. Degradation of (a) threshold voltage ΔV_{th} and (b) gate leakage current I_g/I_{g0} for passivated and unpassivated GaN-based HEMTs. Solid lines refer to passivated devices, while dotted lines refer to unpassivated devices. Irradiations are performed up to 100 Mrad(SiO$_2$), and then devices were annealed at RT for 27 h under similar bias conditions to those applied during irradiation.

all cases except CUT-OFF devices. These show increases of two orders of magnitude, consistent with the stress-induced increase visible in I_{off} in Fig. 12. In passivated devices, the increase of gate leakage is lower than one order of magnitude, regardless of bias applied during irradiation. Since the leakage depends only weakly on gate bias, the leakage in the passivated devices is dominated most likely by charge trapping in the SiN layer [35], [36], while unpassivated devices are most likely dominated by surface trap buildup at the top of the AlGaN [37], [38]. Both the traps in SiN and the surface traps are most likely charged positively after stress, based on the behavior of the device of Fig. 12, and consistent with the electric fields. The comparative responses between the two device types in Fig. 13(b) suggest that the surface trap density in the unpassivated devices exceeds the SiN-charged trap density [23].

VI. Conclusion

AlGaN/GaN HEMTs irradiated at ultrahigh doses show significant degradation due to TID and electrical stress, with magnitudes depending on irradiation bias. In general, ultrahigh doses induce negative V_{th} shifts with magnitudes that are higher than the ones retrieved at lower doses of previous X-rays and gamma studies. The HEMTs irradiated with negative gate bias (OFF-state) exhibit the most negative threshold voltage shifts. At doses $<$10 Mrad(SiO$_2$), TID effects are related to the passivation of pre-existing acceptor-like defects via hole capture, which induces negative threshold voltage shifts and improvement of transconductance. At doses $>$10 Mrad(SiO$_2$), dehydrogenation of defect and impurity complexes leads to the creation of acceptor-like defects. These degrade the transconductance, shift the threshold voltage positively, and increase low-frequency noise. Slight performance recovery is visible after 27 h of RT annealing, most likely due to the formation of a significant density of stable defects.

Irradiation results on passivated and unpassivated HEMTs show that passivation layers may strongly affect oxygen and moisture absorption. The enhanced degradation of unpassivated devices in this study reinforces the key role that oxygen impurities and hydrogen play in the radiation response and long-term reliability of GaN-based HEMTs.

Considering potential system applications, AlGaN/GaN HEMTs have much greater tolerance to ultrahigh doses than Si-based CMOS technologies [1], [2], [9], [12], [15]. In the worst case condition, AlGaN HEMTs show $<$10% ΔI_{on} variation after 100 Mrad(SiO$_2$), which is less than $\sim$38% of 31-nm MOSFETs and $\sim$20% of gate-all-around Si nano-wire FETs, both tested at ultrahigh doses [1], [12]. Hence, the long-term reliability of the AlGaN/GaN HEMTs is likely to be a more limiting factor than their radiation response [15], [18], [20].

References

[1] S. Bonaldo et al., "Ionizing-radiation response and low-frequency noise of 28-nm MOSFETs at ultra-high doses," *IEEE Trans. Nucl. Sci.*, vol. 67, no. 7, pp. 1302–1311, Jul. 2020.

[2] F. Faccio et al., "Radiation-induced short channel (RISCE) and narrow channel (RINCE) effects in 65 and 130 nm MOSFETs," *IEEE Trans. Nucl. Sci.*, vol. 62, no. 6, pp. 2933–2940, Dec. 2015.

[3] S. Bonaldo et al., "Charge buildup and spatial distribution of interface traps in 65-nm pMOSFETs irradiated to ultrahigh doses," *IEEE Trans. Nucl. Sci.*, vol. 66, no. 7, pp. 1574–1583, Jul. 2019.

[4] F. Faccio et al., "Influence of LDD spacers and H^+ transport on the total-ionizing-dose response of 65-nm MOSFETs irradiated to ultrahigh doses," *IEEE Trans. Nucl. Sci.*, vol. 65, no. 1, pp. 164–174, Jan. 2018.

[5] S. Gerardin et al., "Impact of 24-GeV proton irradiation on 0.13-μm CMOS devices," *IEEE Trans. Nucl. Sci.*, vol. 53, no. 4, pp. 1917–1922, Aug. 2006.

[6] C.-M. Zhang et al., "Characterization of GigaRad total ionizing dose and annealing effects on 28-nm bulk MOSFETs," *IEEE Trans. Nucl. Sci.*, vol. 64, no. 10, pp. 2639–2647, Oct. 2017.

[7] S. Bonaldo et al., "Influence of halo implantations on the total ionizing dose response of 28-nm pMOSFETs irradiated to ultrahigh doses," *IEEE Trans. Nucl. Sci.*, vol. 66, no. 1, pp. 82–90, Jan. 2019.

[8] S. Mattiazzo et al., "Total ionizing dose effects on a 28 nm hi-K metal-gate CMOS technology up to 1 Grad," *J. Instrum.*, vol. 12, no. 2, Feb. 2017, Art. no. C02003.

[9] T. Ma et al., "TID degradation mechanisms in 16 nm bulk FinFETs irradiated to ultra-high doses," *IEEE Trans. Nucl. Sci.*, vol. 68, no. 8, pp. 1571–1578, Aug. 2021.

[10] T. Ma et al., "Influence of fin and finger number on TID degradation of 16 nm bulk FinFETs Irradiated to ultrahigh doses," *IEEE Trans. Nucl. Sci.*, vol. 69, no. 3, pp. 307–313, Mar. 2022.

[11] S. Bonaldo et al., "DC response, low-frequency noise, and TID-induced mechanisms in 16-nm FinFETs for high-energy physics experiments," *Nucl. Instrum. Methods Phys. Res. A, Accel. Spectrom. Detect. Assoc. Equip.*, vol. 1033, Jun. 2022, Art. no. 166727.

[12] S. Bonaldo et al., "TID effects in highly scaled gate-all-around Si nanowire CMOS transistors irradiated to ultra-high doses," *IEEE Trans. Nucl. Sci.*, vol. 69, no. 7, pp. 1444–1452, Jul. 2022.

[13] E. C. H. Kyle, S. W. Kaun, P. G. Burke, F. Wu, Y.-R. Wu, and J. S. Speck, "High-electron-mobility GaN grown on free-standing GaN templates by ammonia-based molecular beam epitaxy," *J. Appl. Phys.*, vol. 115, no. 19, May 2014, Art. no. 193702.

[14] A. Lonascut-Nedelscu, C. Carlone, A. Houdayer, H. J. von Bardeleben, and J. L. Cantin, "Radiation hardness of gallium nitride," *IEEE Trans. Nucl. Sci.*, vol. 49, no. 6, pp. 2733–2738, Dec. 2002.

[15] D. M. Fleetwood, E. X. Zhang, R. D. Schrimpf, and S. T. Pantelides, "Radiation effects in AlGaN/GaN HEMTs," *IEEE Trans. Nucl. Sci.*, vol. 69, no. 5, pp. 1105–1119, May 2022.

[16] R. Jiang et al., "Worst-case bias for proton and 10-keV X-ray irradiation of AlGaN/GaN HEMTs," *IEEE Trans. Nucl. Sci.*, vol. 64, no. 1, pp. 218–225, Jan. 2017.

[17] R. Jiang et al., "Dose-rate dependence of the total-ionizing-dose response of GaN-based HEMTs," *IEEE Trans. Nucl. Sci.*, vol. 66, no. 1, pp. 170–176, Jan. 2019.

[18] J. Chen et al., "Effects of applied bias and high field stress on the radiation response of GaN/AlGaN HEMTs," *IEEE Trans. Nucl. Sci.*, vol. 62, no. 6, pp. 2423–2430, Dec. 2015.

[19] T. Roy et al., "Electrical-stress-induced degradation in AlGaN/GaN high electron mobility transistors grown under gallium-rich, nitrogen-rich, and ammonia-rich conditions," *Appl. Phys. Lett*, vol. 96, no. 13, Mar. 2010, Art. no. 133503.

[20] R. Jiang et al., "Multiple defects cause degradation after high field stress in AlGaN/GaN HEMTs," *IEEE Trans. Device Mater. Rel.*, vol. 18, no. 3, pp. 364–376, Sep. 2018.

[21] R. Jiang et al., "Degradation and annealing effects caused by oxygen in AlGaN/GaN high electron mobility transistors," *Appl. Phys. Lett.*, vol. 109, no. 2, Jul. 2016, Art. no. 023511.

[22] S. W. Kaun, M. H. Wong, U. K. Mishra, and J. S. Speck, "Molecular beam epitaxy for high-performance Ga-face GaN electron devices," *Semiconductor Sci. Technol.*, vol. 28, no. 7, Jun. 2013, Art. no. 074001.

[23] R. Jiang et al., "Total ionizing dose effects in passivated and unpassivated AlGaN/GaN HEMTs," in *Proc. RADECS*, Bremen, Germany, Sep. 2016, pp. 1–4.

[24] A. Dasgupta, D. M. Fleetwood, R. A. Reed, R. A. Weller, and M. H. Mendenhall, "Effects of metal gates and back-end-of-line materials on X-ray dose in HfO_2 gate oxide," *IEEE Trans. Nucl. Sci.*, vol. 58, no. 6, pp. 3139–3144, Dec. 2011.

[25] A. Dasgupta, D. M. Fleetwood, R. A. Reed, R. A. Weller, M. H. Mendenhall, and B. D. Sierawski, "Dose enhancement and reduction in SiO_2 and high-κ MOS insulators," *IEEE Trans. Nucl. Sci.*, vol. 57, no. 6, pp. 3463–3469, Dec. 2010.

[26] S. K. Dixit et al., "Radiation induced charge trapping in ultrathin HfO_2-based MOSFETs," *IEEE Trans. Nucl. Sci.*, vol. 54, no. 6, pp. 1883–1890, Dec. 2007.

[27] M. R. Shaneyfelt, D. M. Fleetwood, J. R. Schwank, and K. L. Hughes, "Charge yield for 10-keV X-ray and cobalt-60 irradiation of MOS devices," *IEEE Trans. Nucl. Sci.*, vol. 38, no. 6, pp. 1187–1194, Dec. 1991.

[28] P. F. Wang et al., "Worst-case bias for high voltage, elevated-temperature stress of AlGaN/GaN HEMTs," *IEEE Trans. Device Mater. Rel.*, vol. 20, no. 2, pp. 420–428, Jun. 2020.

[29] J. Chen et al., "Proton-induced dehydrogenation of defects in AlGaN/GaN HEMTs," *IEEE Trans. Nucl. Sci.*, vol. 60, no. 6, pp. 4080–4086, Dec. 2013.

[30] D. M. Fleetwood, "1/f noise and defects in microelectronic materials and devices," *IEEE Trans. Nucl. Sci.*, vol. 62, no. 4, pp. 1462–1486, Aug. 2015.

[31] D. M. Fleetwood, "Total-ionizing-dose effects, border traps, and 1/f noise in emerging MOS technologies," *IEEE Trans. Nucl. Sci.*, vol. 67, no. 7, pp. 1216–1240, Jul. 2020.

[32] P. Wang et al., "1/f noise in as-processed and proton-irradiated GaN/AlGaN HEMTs due to carrier-number fluctuations," *IEEE Trans. Nucl. Sci.*, vol. 64, no. 1, pp. 181–189, Jan. 2017.

[33] G. Ghibaudo, O. Roux, C. Nguyen-Duc, F. Balestra, and J. Brini, "Improved analysis of low frequency noise in field-effect MOS transistors," *Phys. Status Solidi A*, vol. 124, no. 2, pp. 571–581, Apr. 1991.

[34] J. H. Scofield, N. Borland, and D. M. Fleetwood, "Reconciliation of different gate-voltage dependencies of 1/f noise in n-MOS and p-MOS transistors," *IEEE Trans. Electron Devices*, vol. 41, no. 11, pp. 1946–1952, Dec. 1994.

[35] J. W. Chung, J. C. Roberts, E. L. Piner, and T. Palacios, "Effect of gate leakage in the subthreshold characteristics of AlGaN/GaN HEMTs," *IEEE Electron Device Lett.*, vol. 29, no. 11, pp. 1196–1198, Nov. 2008.

[36] N. Xu et al., "Gate leakage mechanisms in normally off p-GaN/AlGaN/GaN high electron mobility transistors," *Appl. Phys. Lett.*, vol. 113, no. 15, Oct. 2018, Art. no. 152104.

[37] H. Yu et al., "Leakage mechanism in ion implantation isolated AlGaN/GaN heterostructures," *J. Appl. Phys.*, vol. 131, no. 3, Jan. 2022, Art. no. 035701.

[38] D. K. Sahoo, R. K. Lal, H. Kim, V. Tilak, and L. F. Eastman, "High-field effects in silicon nitride passivated GaN MODFETs," *IEEE Trans. Electron Devices*, vol. 50, no. 5, pp. 1163–1170, May 2003.

Open Access funding provided by 'Università degli Studi di Padova' within the CRUI CARE Agreement